Influence of the characteristics of soluble algal organic matter released from *Microcystis aeruginosa* on the fouling of a ceramic microfiltration membrane

By

Xiaolei Zhang, Linhua Fan*, Felicity A. Roddick

School of Civil, Environmental and Chemical Engineering, RMIT University,

GPO Box 2476, Melbourne, VIC 3001, Australia

* *Corresponding author. Tel.: +613 9925 3692; fax: +613 9925 3746.*

E-mail address: linhua.fan@rmit.edu.au

Submitted to

Journal of Membrane Science

17th September, 2012

Abstract

The influence of the characteristics of soluble algal organic matter (AOM) on the fouling of a 7-channel tubular ceramic microfiltration membrane (ZrO_2-TiO_2, 0.1 μm) was investigated at lab scale. The AOM (~3 mg DOC/L) extracted from a *Microcystis aeruginosa* culture at three phases of growth (10, 20 and 35 days) all caused severe flux decline, and its fouling potential increased with increasing growth time. Size exclusion chromatography, fluorescence excitation-emission matrix spectra and organic matter fractionation showed that the high MW biopolymers were the major component determining the severity of the AOM fouling of the ceramic membrane. For the AOM at stationary phase (35 days), 0.45 and 1 μm pre-filtration gave greater flux decline and hydraulically irreversible fouling than 5 μm pre-filtration due to the denser foulant layer formed and greater amounts of small organic molecules entering membrane pores. However, the non-pre-filtered AOM (with algal cells) caused the greatest flux decline which was likely due to the presence of the high fouling potential cell surface organic matter. The addition of calcium to the feed solutions led to a marked improvement in flux and reduction in membrane irreversible fouling due to the lower fouling potential of the AOM-calcium complexes formed.

Keywords: Algal organic matter; Ceramic membrane; Characterisation; Fouling; Microfiltration

1. Introduction

Low pressure membrane processes such as microfiltration (MF) and ultrafiltration (UF) are being widely used for the purification of drinking water and wastewater treatment due to their high cost-effectiveness [1]. The use of ceramic MF and UF membranes for water treatment has become popular in recent years as the ceramic membranes possess many advantages over conventional polymeric membranes, such as higher selectivity, higher mechanical and chemical stability, and higher hydrophilicity [2]. However, membrane fouling remains a major drawback for most of the membrane-mediated water treatment processes, since it can lead to substantial losses of product water flux over time and the consequent great reduction in the efficiency of the treatment systems [3].

Blooms of cyanobacteria (also termed blue green algae) such as *Microcystis aeruginosa* in increasingly eutrophic aquatic systems have become a serious environmental issue worldwide. The blooms in natural surface water and treated wastewater can result in a large amount of soluble algal organic matter (AOM) entering downstream water treatment systems [4]. The algal organic compounds are commonly dominated by hydrophobic proteins and hydrophilic polysaccharides which have been widely regarded as responsible for the significant fouling issues in membrane filtration processes [5]. It has been demonstrated that the presence of AOM associated with natural organic matter in surface water or effluent organic matter in wastewater can further reduce the flux of polymeric MF/UF membranes [6-8]. Some efforts have been made since to characterise the AOM fouling of the polymeric MF/UF membranes, with a view to understanding the fouling mechanisms. Qu et al. [9] investigated the influence of the interfacial characteristics of AOM extracted from *M. aeruginosa* including surface charge, molecular size and hydrophilicity on the fouling of UF polymeric membranes. They also studied the impact of the AOM and algal cells on membrane fouling, and reported that the AOM caused greater flux decline than algal cells due to greater pore plugging and less porous cake layer formed by the AOM [10]. It was

found in a further study by the research group that the dissolved AOM could cause greater flux decline but less irreversible membrane fouling compared with cell surface AOM. They suggested that this was because the cell surface AOM contained more large and hydrophobic molecules, which could result in the foulant layer being more porous but having a higher affinity to the membrane surface than dissolved AOM [11]. In another study, Huang et al. [12] observed that different AOM compositions due to different nutrient conditions had different impacts on the fouling of the polymeric MF membranes. The high fouling potential of AOM was attributed to the high molecular weight polysaccharide-like and proteinaceous substances.

Although great attention has been drawn to the application of ceramic membranes in water and wastewater treatment, the information regarding AOM fouling of these membranes is very limited to date. A better understanding of AOM fouling of ceramic membranes (which are significantly different from polymeric membranes in terms of physical, chemical and mechanical properties) is essential for the effective design and operation of the processes. As such, the aim of this study was to investigate the impact of the characteristics of soluble AOM on the fouling of a commercially available ceramic MF membrane at lab scale. The influence of the AOM from different phases of *M. aeruginosa* growth, feed solution pre-filtration, and the presence of calcium ions on the fouling was investigated. Advanced organic matter characterisation techniques including size exclusion chromatography (SEC) using liquid chromatography with organic carbon detection (LC-OCD), fluorescence excitation-emission matrix (EEM) spectra and fractionation using resin adsorption chromatography were employed to gain a better insight into the characteristics of the organic compounds involved.

2. Experimental

2.1. Cultivation of algae, AOM extraction and preparation of feed solutions

M. aeruginosa (CS 566/01-A01) was purchased from the CSIRO Microalgae Research Centre (Tasmania, Australia). The algal cultures were grown in 5 L Schott bottles at 22 ^{o}C using MLA medium [13] under humidified aeration. A 16/8 hour light/dark cycle was used to simulate natural light conditions. According to several reports, the algae have high absorbance at 684 nm [14-16]. Optical density (OD) of the algal cell suspension was therefore used to measure algal cell concentration. The correlation between OD_{684} and cell count (5×10^3 - 5×10^6 cells mL^{-1}) was verified as indicated by their strong linear relationship ($R^2 > 0.99$) (data not shown).

Algal cultures were harvested at the 10th (early exponential phase), 20th (late exponential phase) and 35th day (stationary phase) of growth. Centrifugation (3270 × g for 30 mins) of the algal cell suspensions and the subsequent filtration of the supernatant (using 1 µm membranes unless otherwise stated) were conducted to extract the dissolved extracellular AOM [8, 9]. In the preparation of the MF feed solutions, the extracted AOM was diluted to approximately the same dissolved organic carbon (DOC) concentration (5.0 ± 0.2 mg/L) with tap water (1.9 ± 0.05 mg DOC/L). The pH of the MF feed solution was adjusted to 8.0 ± 0.2 using 1 M HCl or 1 M NaOH prior to each filtration run.

2.2. Ceramic membrane filtration rig

A 7-channel tubular ceramic ZrO_2-TiO_2 MF membrane with a nominal pore size of 0.1 µm (CeRAM^{TM} INSIDE, TAMI Industries) was used in the filtration experiments. The active layer of this membrane is made of a mixture of ZrO_2 and TiO_2, and the support layer is made of TiO_2. These materials give the membrane a highly hydrophilic nature which can reduce the fouling potential to some extent. According to the manufacturer, the membrane can be operated at high temperature (up to 350 ^{o}C) and is insensitive to bases and acids. A

schematic diagram of the lab-scale ceramic membrane system is presented in Fig. 1. The rig can be operated in either dead-end or cross-flow mode by closing or opening the downstream valve (Valve 3). All filtration runs were carried out in inside-out and dead-end modes at a constant transmembrane pressure (TMP) of 70 ± 1 kPa and under room temperature (22 ± 2 ^{o}C). Membrane backwashing was carried out by filtering tap water in outside-in operation mode (i.e., closing Valves 1 and 4, opening Valves 2 and 3) at the same TMP as the filtration runs.

Fig. 1. Schematic diagram of the ceramic membrane filtration system, P1, P2, P3 are manometers.

2.3. Microfiltration test

Prior to each MF run, the clean water flux of the clean membrane (J_0) was obtained by filtering tap water for 2 minutes. The AOM solution was then filtered for 90 minutes under the defined conditions. Membrane permeate flow rate was recorded continuously, and the permeate was sampled after 15, 30, 60 and 90 minutes filtration for chemical analyses. After AOM solution filtration, the clean water flux of the fouled membrane (J_a) was determined by filtering tap water for 2 minutes. The membrane was then backwashed for 2 minutes, and the clean water flux of the backwashed membrane (J_b) was measured by filtering tap water for 2 minutes. Reversible fouling (RF), an indicator of the affinity of foulant for the membrane, was estimated using the following equation (Eq. (1)) [17]. The series resistances including reversible (R_r) and irreversible filtration resistance (R_i) were also calculated using the method described elsewhere [18].

$$RF = \frac{J_b - J_a}{J_0 - J_a} \times 100\% \quad (1)$$

The same membrane was used for all MF runs, and after each run the membrane was restored by Cleaning in Place (CIP) until the permeate flux reached 138-148 LMH. CIP was carried out through the following steps: 1) 0.1M NaOH solution (65 ^{o}C) for 30 minutes; 2) 0.1M HNO_3 solution (65 ^{o}C) for 20 minutes; 3) tap water (18 - 20 ^{o}C) for 2 minutes. All filtration tests were run in duplicate. As the final flux of the duplicate tests typically agreed within 5% and the trend was found to be consistent between the duplicate runs, only one set of flux data was reported. Reversible fouling results were reported using average values.

2.4. Analytical methods

DOC was determined using a Sievers 820 TOC analyser. UVA_{254} and OD_{684} were measured using a UV/vis spectrophotometer (UV2, Unicam). The pH was measured using a Hach Sension 156 pH meter. The concentration of calcium was measured with an atomic absorption spectrometer (AA240FS, Varian). Apparent molecular weight distribution of the AOM was determined by SEC with LC-OCD at the Water Research Centre of the University of New South Wales, Sydney, Australia. The LC-OCD system (LC-OCD Model 8, DOC-Labor Dr. Huber, Germany) utilised a SEC column (Toyopearl TSK HW-50S, diameter 2 cm, length 25 cm) and the chromatograms were processed using the Labview based program Fiffikus (DOC-Labor Dr. Huber, Germany). Fluorescence excitation-emission matrix (EEM) spectra were obtained using a fluorescence spectrometer (LS 55, PerkinElmer) at an excitation and emission wavelength range of 200–550 nm. In order to remove the Raman scatter and other background noise, the fluorescence spectra of Milli-Q water were subtracted from all EEM spectra using Origin software. Fractionation using XAD-4 and DAX-8 resins was used to separate the organics into hydrophobic (HPO), transphilic (TPI), and hydrophilic (HPI) fractions [19].

3. Results and discussion

3.1. Influence of AOM from different phases of *M. aeruginosa* growth

3.1.1. Flux decline and reversibility of AOM fouling

Rapid flux decline was observed during the MF of the solutions containing the AOM extracted at 10, 20 and 35 days of *M. aeruginosa* growth, with the majority of flux decline occurring before the specific permeate volume reached 30 L/m^2 (Fig. 2). In the initial stage of the filtration (< 30 L/m^2), the solution containing Day 35 AOM gave a much more rapid and greater flux reduction compared with Day 10 and Day 20 AOM. The maximum flux decline was reached at about 40 L/m^2 for the Day 35 AOM, whereas Day 10 and Day 20 AOM solutions led to continued flux reduction until the runs were terminated. On reaching 80 L/m^2, Day 20 AOM exhibited a similar flux to Day 35 AOM, which was about 5% greater than Day 10 AOM. Control filtration tests with tap water and MLA solution (the concentration of MLA in tap water was the same as that in the Day 10 AOM solution) showed the flux decline was relatively insignificant compared with the AOM solutions. The impact of the organic matter in the tap water and MLA on the membrane performance was therefore considered negligible in this study.

The extent of reversible fouling by the AOM decreased with increasing *M. aeruginosa* growth time, with 35% for Day 10 (R_r 39.4×10^{10} m^{-1}, R_i 48.9×10^{10} m^{-1}), 17% for Day 20 (R_r 27.7×10^{10} m^{-1}, R_i 82.8×10^{10} m^{-1}) and 10% for Day 35 (R_r 18.3×10^{10} m^{-1}, R_i 103.9×10^{10} m^{-1}). Hence the AOM obtained from a later phase of algal growth had higher affinity for the ceramic membrane compared with the AOM from an earlier growth phase, and consequently led to more severe irreversible membrane fouling.

.

Fig. 2. Normalized flux vs. specific volume for the MF of tap water, MLA solution and the solutions containing AOM from different phases of *M. aeruginosa* growth.

3.1.2. AOM rejection by the ceramic MF membrane

DOC rejection for the AOM from the three phases of *M. aeruginosa* growth was similar (31-35%), and the DOC rejection for each AOM sample was fairly consistent (variation 2-4%) over the filtration period (Fig. 3). A similar trend was observed for UVA_{254} rejection (16-20%), however the UVA rejection was markedly lower than DOC rejection. This indicated that the organic matter retained by the membrane contained less UV-absorbing organic materials. As suggested by Zheng et al. [20], the retained organic matter could contain a large portion of biopolymer substances in the AOM, such as proteins and polysaccharides.

Fig. 3. DOC and UVA_{254} rejection during MF of the three AOM solutions.

3.1.3. Characterisation of the AOM by LC-OCD

In order to interpret the diverse fouling behaviour of the AOM from the different phases of algal growth, the molecular weight distribution of the AOM was examined using SEC with LC-OCD (Fig. 4). Day 10 AOM contained significantly less high MW organic components such as biopolymers (> 20,000 Da) and humic-like substances (500-20,000 Da), but more medium-MW components (i.e., building blocks, 350-500 Da), low MW acids and low MW humic substances (< 350 Da) compared with Day 20 and Day 35 AOM. Although Day 35 AOM had a similar content of biopolymers and low-MW compounds to the Day 20 AOM, it contained significantly more humic-like substances.

Biopolymers such as polysaccharides and proteins have been proven to result in severe fouling of polymeric MF membranes [1, 21]. On the other hand, the deposition of humic substances via hydrophobic interaction with the surface of membranes can also lead to significant membrane fouling [22]. The flux and reversible fouling results presented in section 3.1.2 were therefore related to the relative content of the high MW organic compounds (biopolymers and humic-like substances) in the AOM derived from the different phases of algal growth. The lower fouling potential for the AOM from the early exponential phase (Day

10) was due to the lower content of biopolymers and high MW humic-like substances. The greater fouling potential of Day 35 AOM compared with Day 20 AOM was associated with a greater amount of high MW humic-like substances, which could result in an enhanced fouling effect on the membrane as reported by Yuan and Zydney [22]. However, it may also be possible that the different fouling behaviour of the Day 20 and Day 35 AOM was due to the different chemical compositions of their biopolymers.

Fig. 4. LC-OCD chromatograms of the AOM from different phases of *M. aeruginosa* growth. HS = humic substances.

3.1.4. Characterisation of AOM by fluorescence EEM spectra

Fluorescence EEM spectra are widely used for the characterisation of fluorescent organic components in natural organic matter or wastewater effluent organic matter. According to Chen et al. [23], EEM spectra can be divided into 5 regions (Fig. 5a). Regions I (Ex/Em: 220-270 nm/280-330 nm) and II (Ex/Em: 220-270 nm/330-380 nm) correspond to aromatic proteins, and region III (Ex/Em: 220-270 nm/380-540 nm) is associated with fulvic acid (FA)-like substances. Regions IV (Ex/Em: 270-440 nm/280-380 nm) and V (Ex/Em: 270-440 nm/380-540 nm) represent soluble microbial products (SMPs, e.g., proteins and polysaccharide-like materials) and humic acid (HA)-like materials, respectively. The AOM extracts for the different phases of *M. aeruginosa* growth exhibited different EEM spectral features (Figs. 5a, b & c). The fluorophores increased with increasing *M. aeruginosa* growth time in all EEM regions, which was likely due to the changes in molecular weight/size distribution and/or chemical composition of the AOM over the algal growth phases, i.e., from lower MW to higher MW as shown in Fig. 4. There was a marked increase in fluorescence for all regions between the late exponential (20 days) and the stationary phase (35 days) (Figs. 5b & c).

The fluorescence regional integration (FRI) method [23] was used to quantify the changes in the fluorescent organic species before and after the MF runs in terms of EEM spectra (EEMs) volume in each region (Fig. 6). The EEMs volumes of the tap water before and after MF are provided as a reference. The EEMs volumes for the HA-like and FA-like regions of the organic matter in Day 10 AOM solution was mainly contributed by the organic matter in the tap water, whereas almost all of the aromatic proteins (AP) and SMPs in the solution were contributed by the AOM. After MF, the reductions in EEMs volume in all five regions for Day 10 AOM were markedly lower than for Day 20 and Day 35 AOM. This suggested that less organic matter associated with these regions for the Day 10 AOM was retained by the membrane, and hence led to less fouling of the membrane. The lower rejection of these fluorescent organic components was attributed to the relative abundance of low MW compounds in the early phase of *M. aeruginosa* growth (Fig. 4). There were considerably greater reductions in EEMs volumes in both the AP and SMPs regions for Day 35 AOM and Day 20 AOM (i.e., 66% and 39% for AP, 38% and 24% for SMPs, respectively) compared with the reductions in the FA-like and HA-like regions (i.e., 34% and 18% for FA-like, 18% and 5% for HA, respectively). This indicated that aromatic proteins and SMP-like substances were the major fouling organic components of the ceramic MF membrane. It should be noted that a considerably greater amount of humic substances in the Day 35 AOM was retained by the membrane compared with Day 20 AOM, this could also play a role in the enhanced membrane fouling for the Day 35 AOM.

Fig. 5. Fluorescence EEM spectra of (a) Day 10, (b) Day 20 and (c) Day 35 AOM. Region I and II: aromatic proteins (AP); Region III: fulvic acid-like (FA); Region IV: soluble microbial products (SMPs); Region V: humic acid-like (HA)

Fig. 6. EEM spectra volumes for the AOM before and after MF.

3.1.5. AOM fractionation

The AOM before and after microfiltration was fractionated into different organic groups using resin adsorption chromatography, and the results are presented in Fig. 7 in terms of DOC concentrations. Day 10 AOM contained significantly more hydrophobic (HPO) but less transphilic compounds (TPI), and its hydrophilic fraction (HPI) was only slightly lower than Day 20 and 35 AOM. Although the rejection of bulk DOC was similar for the three AOM samples (Fig. 3), the rejection of their fractions varied significantly. There were greater reductions in HPO (38%) and TPI (34%) fractions for the Day 10 AOM after MF compared with Day 20 (29% HPO and 19% TPI) and Day 35 AOM (33% HPO and 23% TPI). However, there was significantly less reduction in HPI (29%) for Day 10 AOM compared with Day 20 and Day 35 AOM which had 46 and 63% reduction, respectively. The results suggested that HPI had greater fouling potential than the HPO and TPI fractions, as the greater retention of HPO and TPI for Day 10 AOM did not result in poorer membrane performance compared with Day 20 or Day 35 AOM. This was consistent with some previous studies where the hydrophilic organic fraction that contained a greater proportion of high MW compounds such as biopolymers was found to have higher fouling potential compared with hydrophobic (such as humic substances) and transphilic compounds [1, 18].

Although the HPI content was only slightly higher for Day 35 AOM than Day 10 and Day 20 AOM, there was a markedly greater retention of this fraction for the Day 35 AOM (63% cf. 46% Day 20 and 29% Day 10). This indicated that the composition/physico-chemical properties of the HPI fractions in the three AOM samples were markedly different, and hence they exhibited different fouling behaviour. It has been reported that the AOM derived from the stationary phase of *M. aeruginosa* contained more hydrophilic biopolymer substances (i.e., hydrophilic proteins and carbohydrates) compared with the AOM in the exponential growth phase [24]. Therefore, the increased fouling by the AOM derived from a later algal growth phase in our study was attributed to the hydrophilic biopolymers, which had greater fouling potential compared with the other fractional components in the AOM.

Fig. 7. Fractional components of AOM in MF feed and permeate. HPO: hydrophobic fraction; TPI: transphilic fraction; HPI: hydrophilic fraction.

3.2. Influence of AOM pre-filtration

The impact of pre-filtration of the AOM on the fouling of the ceramic MF membrane was studied by comparing the flux decline and reversible fouling for 0.45, 1 and 5 μm pre-filtered AOM and non-pre-filtered AOM (with *M. aeruginosa* cells) (Fig. 8). The AOM after 5 μm pre-filtration gave significantly less flux reduction during the whole filtration period compared with the other feed solutions. It was observed that around 70% of the algal cells were removed by 5 μm pre-filtration (data not shown), and the lower flux reduction for the 5 μm pre-filtered AOM indicated that the remaining particulates (including the smaller algal cells) formed a fouling layer with lower filtration resistance. The 0.45 and 1 μm filtered AOM caused a similar flux decline over the filtration period, which was likely due to these two pre-filtration membranes being relatively similar in pore size and hence their filtrates would have similar physico-chemical properties. However, the non-pre-filtered AOM produced the greatest flux decline which suggested that the algal cell-AOM and/or cell-membrane interactions could have played an influential role in the fouling of the ceramic MF membrane.

The above results imply that both dissolved AOM (< 0.45 or 1 μm) and the particulates in the AOM solutions can affect the filtration process. The dissolved AOM can cause much more rapid and greater flux decline due to the resultant denser fouling layer, and the presence of particulates can alleviate the initial rapid flux decline due to the formation of a more porous layer of lower resistance. However, the particulates can build up on the membrane surface and make the fouling layer thicker as the filtration proceeds, and hence increase the filtration resistance, leading to greater further reduction in flux at the later stage of filtration (e.g., after 40 L/m^2 for the 5 μm pre-filtered AOM). In addition, the AOM attached to the algal cells

(also termed cell surface AOM or bound extracellular organic matter) could cause linkages between the cells, leading to a more compact cake layer under the system pressure and hence greater reduction in flux [25].

Fig. 8. Normalized flux vs. specific volume for the MF of the solutions of: 1) AOM with cells; 2) 0.45 µm pre-filtered AOM; 3) 1.0 µm pre-filtered AOM; 4) 5.0 µm pre-filtered AOM. (All feed solutions contained AOM extracted from stationary phase)

It was observed that the 5 µm pre-filtered AOM gave the highest reversible fouling (around 21%, R_r 43.9 × 10^{10} m^{-1}, R_i 97.8 × 10^{10} m^{-1}). This was likely due to the loosely bonded "pre-layer" formed by the particulates which can prevent smaller particulates from entering the membrane pores, and hence lead to reduced irreversible fouling. As a comparison, only 8-10% reversible fouling (R_r 24.6 × 10^{10} m^{-1}, R_i 119.9 × 10^{10} m^{-1}) was obtained for the AOM pre-filtered by the 0.45 or 1 µm filters. The non-pre-filtered AOM solution (i.e., with cells) also produced lower reversible fouling (10%, R_r 25.8 × 10^{10} m^{-1}, R_i 128.9 × 10^{10} m^{-1}). This was likely due to the presence of the algal cell surface AOM which was reported to have higher potential for irreversible membrane fouling compared with the dissolved AOM [11].

3.3. Influence of calcium ion

In order to get further insights into the interfacial characteristics of the AOM, calcium (i.e., $CaCl_2$) of different concentrations was added to feed solutions containing stationary phase AOM. Addition of calcium reduced the flux decline markedly (Fig. 9), with 2.5 mM of calcium giving slightly greater flux improvement compared with other dosages. As noted by Qu et al. [9], the addition of calcium increased the AOM molecular sizes due to complexation. A significant amount of calcium was retained by the membrane at all dosages, i.e., 17.5 - 49.7% (Table 1), which indicated the formation of large complexes of calcium ions and the AOM (i.e., > 0.1µm). The large AOM complexes would then form a more porous pre-layer and so result in a higher filtration flux. It was observed that the addition of calcium also led to increased reversible fouling at all calcium dosages (from 11% to 20-25%, R_r from 18.3 × 10^{10}

385 m^{-1} to ~ 43.7 × 10^{10} m^{-1}, R_i from 103.9 × 10^{10} m^{-1} to 77.7 × 10^{10} – 97.8 × 10^{10} m^{-1}). At 10 mM
386 calcium, there was less flux improvement. This was most probably due to the increased
387 amount of AOM-calcium complexes (as indicated by the increased calcium retention at 10
388 mM), which would result in a thicker cake layer and hence higher resistance to the filtration.
389
390 The DOC retained by the ceramic membrane during MF of the feed solution without addition
391 of calcium was slightly higher than the feed with the calcium addition at 1.0, 2.5 or 5.0 mM
392 (Table 1). This was attributed to the denser fouling layer formed by the AOM solution (no
393 calcium addition), which led to the greater retention of some AOM molecules compared with
394 the more porous layer formed by the AOM-calcium complexes. However, the calcium
395 dosage at 10 mM resulted in a greater DOC retention compared with the feed without
396 calcium addition. This could be due to the trapping of some AOM molecules by the resultant
397 thicker fouling layer and/or the increased complexation of the AOM at the high calcium
398 dosage. It is known that at high calcium concentration aquatic organic matter becomes
399 insoluble when maximum complexation is attained [26].
400
401 **Fig. 9.** Normalized flux vs. specific volume for the MF of AOM (stationary phase) solutions
402 with and without addition of calcium.
403
404 **Table 1.** Retention of calcium and DOC by the ceramic MF membrane at different calcium
405 dosages.
406
407
408 **4. Conclusions**
409
410 The influence of the soluble AOM extracted from three different phases of *M. aeruginosa*
411 growth, AOM pre-filtration and the presence of calcium ion on the fouling of a 0.1 μm ZrO_2-
412 TiO_2 ceramic MF membrane was studied. AOM from the different algal growth phases all

caused rapid and great flux decline, but exhibited different fouling potentials, with fouling for the stationary phase > late exponential phase > early exponential phase. Characterisation of the AOM using SEC with LC-OCD, fluorescence EEMs and organic matter fractionation indicated that the biopolymers (containing mainly proteinaceous materials and polysaccharides) were the major organic component that determined the severity of the AOM fouling of the ceramic MF membrane. Since the amount of biopolymer in the late exponential and the stationary phase AOM was fairly similar, it is suggested that a difference in the properties of the biopolymers led to the higher fouling potential of the stationary phase AOM.

For the stationary phase, the soluble AOM (i.e., 0.45 or 1 µm pre-filtered) caused more rapid flux decline compared with the 5 µm pre-filtered AOM. The relatively lower flux decline for the 5 µm pre-filtered AOM was attributed to a more porous foulant layer due to the presence of particulates in the feed solution. However, the non-pre-filtered AOM (with algal cells) produced the greatest flux reduction, which was likely due to the presence of the high fouling potential cell surface organics. The addition of calcium to the AOM solutions led to reduced flux decline and increased reversible fouling due to complexation of the calcium ions with the AOM molecules to form large complexes and consequently a more porous foulant layer on the membrane surface.

The results indicate that monitoring algal growth can be important for the effective prediction of fouling and implementation of maintenance measures for ceramic membrane systems during cyanobacterial bloom events. Removal of cyanobacterial cells by a loose MF pre-filter (e.g., 5 µm) may mitigate membrane fouling due to the reduction of the cell surface organic matter. Furthermore, chemical coagulation may be an effective pre-treatment of AOM containing water for improving the filtration performance of the ceramic MF membranes since the fouling potential of AOM can be greatly reduced by its complexation with metal ions.

441

442 **References**

443

444 [1] N. Lee, G. Amy, J.-P. Croué, H. Buisson, Identification and understanding of fouling in
445 low-pressure membrane (MF/UF) filtration by natural organic matter (NOM), Water Res.
446 38 (2004) 4511-4523.
447 [2] B. Hofs, J. Ogier, D. Vries, E.F. Beerendonk, E.R. Cornelissen, Comparison of ceramic
448 and polymeric membrane permeability and fouling using surface water, Sep. Purif.
449 Technol. 79 (2011) 365-374.
450 [3] P. Bacchin, P. Aimar, R.W. Field, Critical and sustainable fluxes: Theory, experiments
451 and applications, J. Membr. Sci. 281 (2006) 42-69.
452 [4] J. Fang, X. Yang, J. Ma, C. Shang, Q. Zhao, Characterization of algal organic matter and
453 formation of DBPs from chlor(am)ination, Water Res.44 (2010) 5897-5906.
454 [5] Y.-T. Chiou, M.-L. Hsieh, H.-H. Yeh, Effect of algal extracellular polymer substances on
455 UF membrane fouling, Desalination 250 (2010) 648-652.
456 [6] N. Lee, G. Amy, J.-P. Croué, Low-pressure membrane (MF/UF) fouling associated with
457 allochthonous versus autochthonous natural organic matter, Water Res. 40 (2006) 2357-
458 2368.
459 [7] Y. Goh, J. Harris, F. Roddick, Impact of Microcystis aeruginosa on membrane fouling in a
460 biologically treated effluent, Water Sci. Technol. 63 (2011) 2853-2859.
461 [8] Y. Goh, J. Harris, F. Roddick, Reducing the effect of cyanobacteria in the microfiltration of
462 secondary effluent, Water Sci. Technol. 62 (2010) 1682.
463 [9] F. Qu, H. Liang, Z. Wang, H. Wang, H. Yu, G. Li, Ultrafiltration membrane fouling by
464 extracellular organic matters (EOM) of Microcystis aeruginosa in stationary phase:
465 Influences of interfacial characteristics of foulants and fouling mechanisms, Water Res.
466 46 (2012) 1490-1500.

[10] F. Qu, H. Liang, J. Tian, H. Yu, Z. Chen, G. Li, Ultrafiltration (UF) membrane fouling caused by cyanobateria: Fouling effects of cells and extracellular organics matter (EOM), Desalination 293 (2012) 30-37.

[11] F. Qu, H. Liang, J. He, J. Ma, Z. Wang, H. Yu, G. Li, Characterization of dissolved extracellular organic matter (dEOM) and bound extracellular organic matter (bEOM) of Microcystis aeruginosa and their impacts on UF membrane fouling, Water Res. 46 (2012) 2881-2890.

[12] W. Huang, H. Chu, B. Dong, Characteristics of algogenic organic matter generated under different nutrient conditions and subsequent impact on microfiltration membrane fouling, Desalination 293 (2012) 104-111.

[13] C. Bolch, S. Blackburn, Isolation and purification of Australian isolates of the toxic cyanobacterium *Microcystis aeruginosa* Kütz, J. Appl. Phycol. 8 (1996) 5-13.

[14] P. Rajasekhar, L. Fan, T. Nguyen, F.A. Roddick, Impact of sonication at 20 kHz on Microcystis aeruginosa, Anabaena circinalis and Chlorella sp, Water Res. 46 (2012) 1473-1481.

[15] G. Zhang, P. Zhang, H. Liu, B. Wang, Ultrasonic damages on cyanobacterial photosynthesis, Ultrason. Sonochem. 13 (2006) 501-505.

[16] G. Zhang, P. Zhang, B. Wang, H. Liu, Ultrasonic frequency effects on the removal of Microcystis aeruginosa, Ultrason. Sonochem. 13 (2006) 446-450.

[17] M. Hashino, K. Hirami, T. Katagiri, N. Kubota, Y. Ohmukai, T. Ishigami, T. Maruyama, H. Matsuyama, Effects of three natural organic matter types on cellulose acetate butyrate microfiltration membrane fouling, J. Membr. Sci. 379 (2011) 233-238.

[18] L. Fan, J.L. Harris, F.A. Roddick, N.A. Booker, Influence of the characteristics of natural organic matter on the fouling of microfiltration membranes, Water Res. 35 (2001) 4455-4463.

[19] G.R. Aiken, D.M. McKnight, K.A. Thorn, E.M. Thurman, Isolation of hydrophilic organic acids from water using nonionic macroporous resins, Org. Geochem. 18 (1992) 567-573.

494 [20] X. Zheng, M. Ernst, M. Jekel, Identification and quantification of major organic foulants
495 in treated domestic wastewater affecting filterability in dead-end ultrafiltration, Water Res.
496 43 (2009) 238-244.
497 [21] C.N. Laabs, G.L. Amy, M. Jekel, Understanding the Size and Character of Fouling-
498 Causing Substances from Effluent Organic Matter (EfOM) in Low-Pressure Membrane
499 Filtration, Environ. Sci. Technol. 40 (2006) 4495-4499.
500 [22] W. Yuan, A.L. Zydney, Humic acid fouling during microfiltration, J. Membr. Sci. 157
501 (1999) 1-12.
502 [23] W. Chen, P. Westerhoff, J.A. Leenheer, K. Booksh, Fluorescence Excitation−Emission
503 Matrix Regional Integration to Quantify Spectra for Dissolved Organic Matter, Environ.
504 Sci. Technol. 37 (2003) 5701-5710.
505 [24] R.K. Henderson, A. Baker, S.A. Parsons, B. Jefferson, Characterisation of algogenic
506 organic matter extracted from cyanobacteria, green algae and diatoms, Water Res. 42
507 (2008) 3435-3445.
508 [25] S. Babel, S. Takizawa, Microfiltration membrane fouling and cake behavior during algal
509 filtration, Desalination 261 (2010) 46-51.
510 [26] S. Hong, M. Elimelech, Chemical and physical aspects of natural organic matter (NOM)
511 fouling of nanofiltration membranes, J. Membr. Sci. 132 (1997) 159-181.
512
513
514
515
516
517
518
519
520
521

Table 1. Retention of calcium and DOC by the ceramic MF membrane at different calcium dosages.

Calcium dosage (mM)	Calcium retention (%)	DOC retention (%)
0	-	36.5
1.0	17.5	33.4
2.5	37.0	31.8
5.0	42.5	32.3
10.0	49.7	41.1

Figure Captions

Fig. 8. Schematic diagram of the ceramic membrane filtration system, P1, P2, P3 are manometers.

Fig. 9. Normalized flux vs. specific volume for the MF of tap water, MLA solution and the solutions containing AOM from different phases of *M. aeruginosa* growth.

Fig. 10. DOC and UVA_{254} rejection during MF of the three AOM solutions.

Fig. 11. LC-OCD chromatograms of the AOM from different phases of *M. aeruginosa* growth. HS = humic substances.

Fig. 12. Fluorescence EEM spectra of (a) Day 10, (b) Day 20 and (c) Day 35 AOM. Regions I and II: aromatic proteins (AP); Region III: fulvic acid-like (FA); Region IV: soluble microbial products (SMPs); Region V: humic acid-like (HA)

Fig. 13. EEM spectra volumes for the AOM and tap water before and after MF.

Fig. 14. Fractional components of AOM in MF feed and permeate. HPO: hydrophobic fraction; TPI: transphilic fraction; HPI: hydrophilic fraction.

Fig. 15. Normalized flux vs. specific volume for the MF of the solutions of: 1) AOM with cells; 2) 0.45 µm pre-filtered AOM; 3) 1.0 µm pre-filtered AOM; 4) 5.0 µm pre-filtered AOM. (All feed solutions contained AOM extracted from stationary phase)

Fig. 16. Normalized flux vs. specific volume for the MF of AOM (stationary phase) solutions with and without addition of calcium.

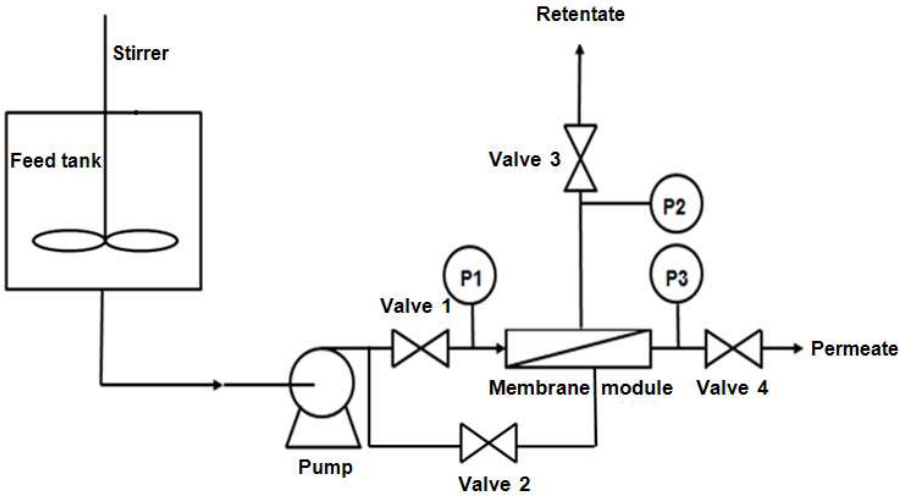

Fig. 1. Schematic diagram of the ceramic membrane filtration system, P1, P2, P3 are manometers.

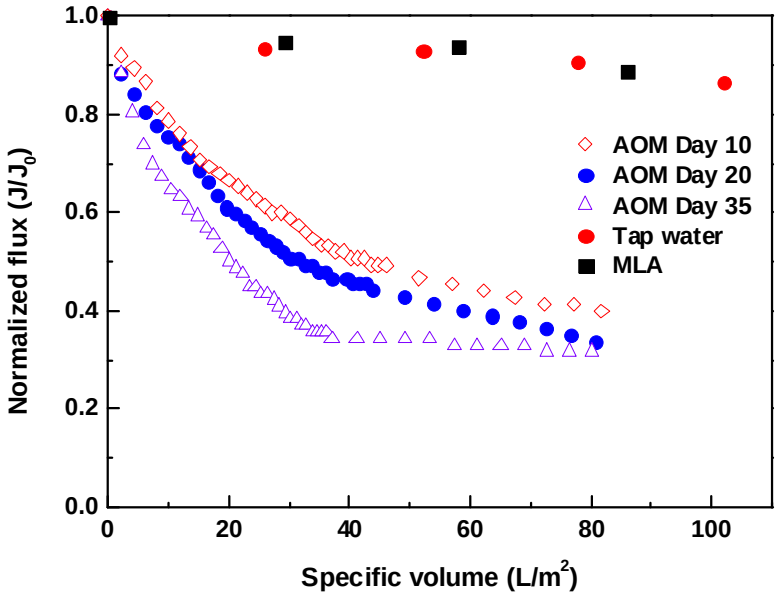

Fig. 2. Normalized flux vs. specific volume for the MF of tap water, MLA solution and the solutions containing AOM from different phases of *M. aeruginosa* growth.

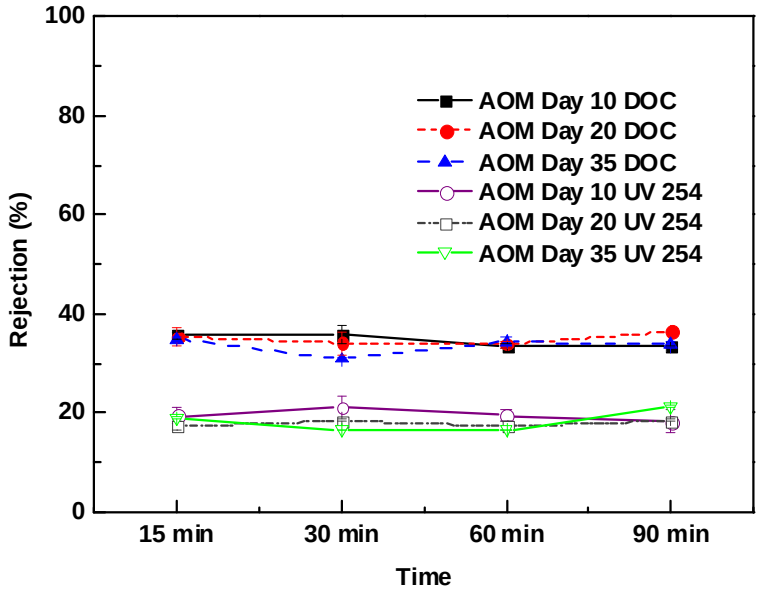

Fig. 3. DOC and UVA_{254} rejection during MF of the three AOM solutions.

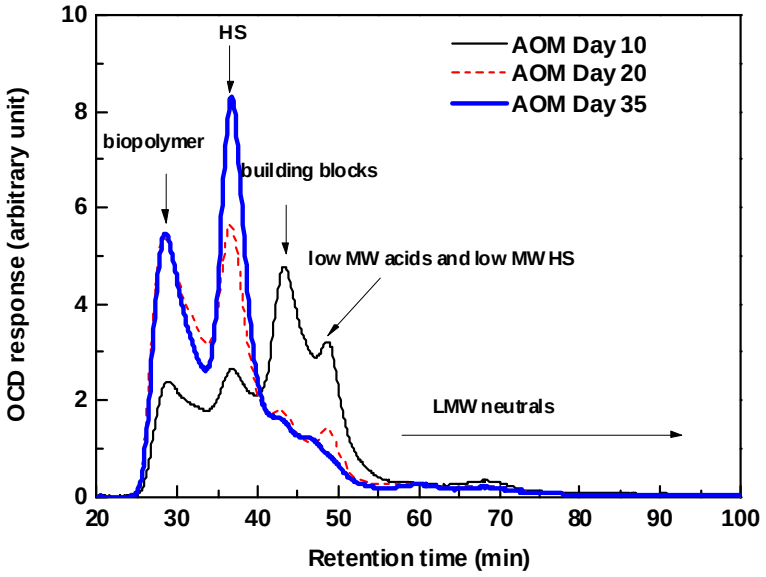

Fig. 4. LC-OCD chromatograms of the AOM from different phases of *M. aeruginosa* growth. HS = humic substances.

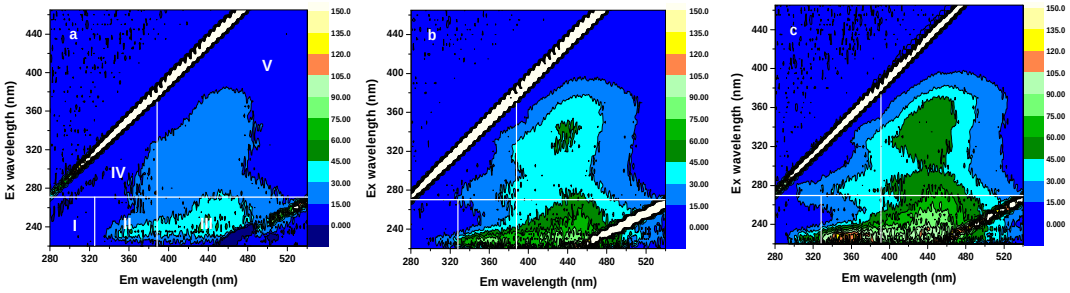

Fig. 5. Fluorescence EEM spectra of (a) Day 10, (b) Day 20 and (c) Day 35 AOM. Regions I and II: aromatic proteins (AP); Region III: fulvic acid-like (FA); Region IV: soluble microbial products (SMPs); Region V: humic acid-like (HA).

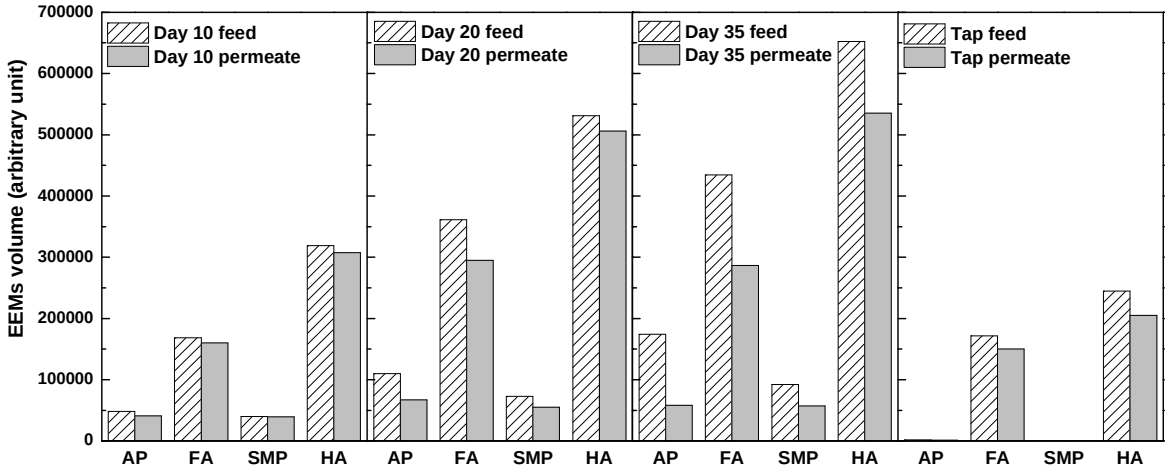

Fig. 6. EEM spectra volumes for the AOM and tap water before and after MF.

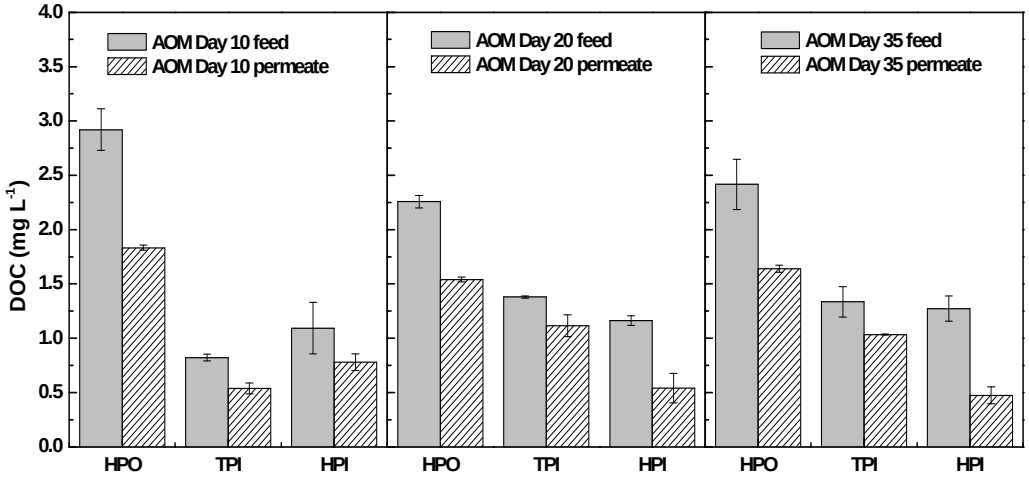

Fig. 7. Fractional components of AOM in MF feed and permeate. HPO: hydrophobic fraction; TPI: transphilic fraction; HPI: hydrophilic fraction.

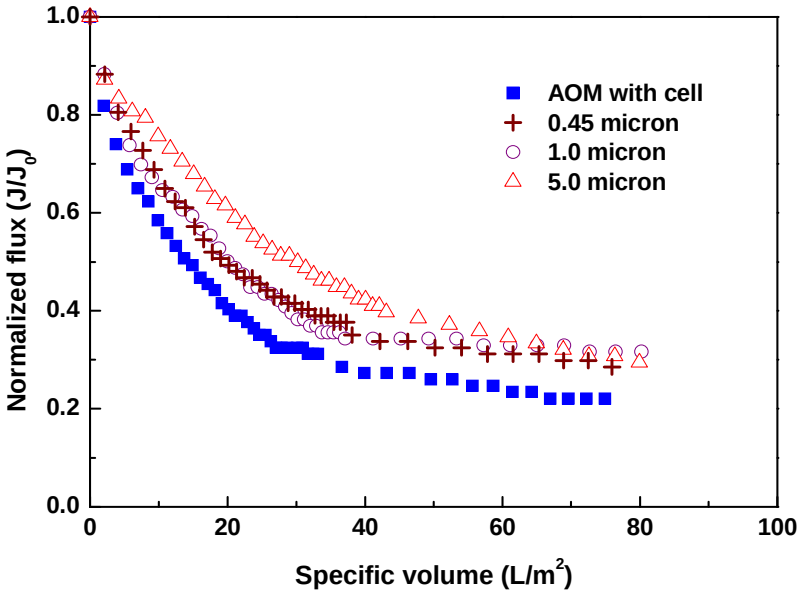

Fig. 8. Normalized flux vs. specific volume for the MF of the solutions of: 1) AOM with cells; 2) 0.45 µm pre-filtered AOM; 3) 1.0 µm pre-filtered AOM; 4) 5.0 µm pre-filtered AOM. (All feed solutions contained AOM extracted from stationary phase)

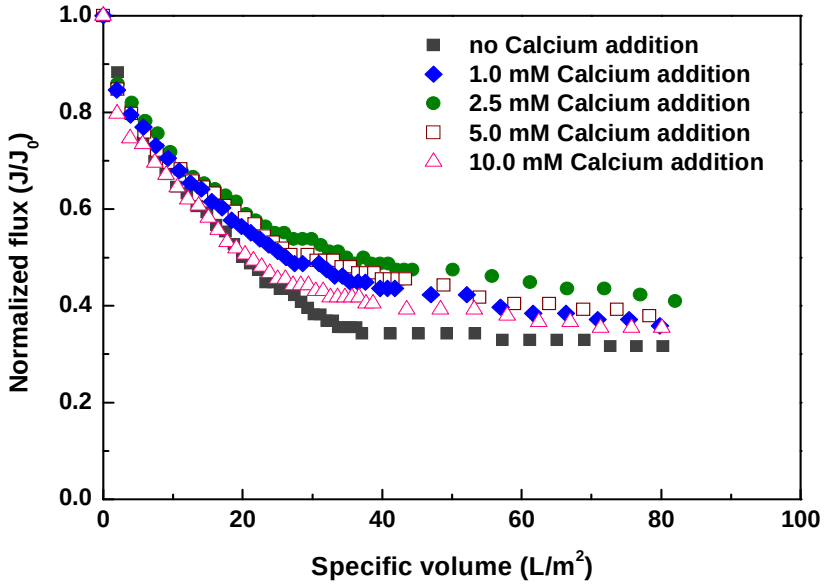

Fig. 9. Normalized flux vs. specific volume for the MF of AOM (stationary phase) solutions with and without addition of calcium.